Ocean Acidification Regulates the Activity, Community Structure, and Functional Potential of Heterotrophic Bacterioplankton in an Oligotrophic Gyre

Xiaomin Xia[1], Yu Wang[2,3], Yunlan Yang[2,3], Tingwei Luo[2,3], Joy D. Van Nostrand[4], Jizhong Zhou[4,5,6], Nianzhi Jiao[2,3], and Rui Zhang[2,3]

[1] Key Laboratory of Tropical Marine Bio-resources and Ecology, South China Sea Institute of Oceanology, Chinese Academy of Sciences, [2] State Key Laboratory of Marine Environmental Science, Xiamen University, [3] Institute of Marine Microbes and Ecospheres, Xiamen University, [4] Institute for Environmental Genomics, Department of Microbiology and Plant Biology, and School of Civil Engineering and Environmental Sciences, University of Oklahoma, Norman, OK, USA, [5] State Key Joint Laboratory of Environment Simulation and Pollution Control, School of Environment, Tsinghua University, Beijing, China, [6] Earth and Environmental Sciences, Lawrence Berkeley National Laboratory, Berkeley, California, USA

Correspondence to: N. Jiao, and R. Zhang, ruizhang@xmu.edu.cn; jiao@xmu.edu.cn

Abstract

Ocean acidification (OA), a consequence of increased global carbon dioxide (CO_2) emissions, is considered a major threat to marine ecosystems. Its effects on bacterioplankton activity, diversity, and community composition have received considerable attention. However, the direct impact of OA on heterotrophic bacterioplankton is often masked by the significant response of phytoplankton due to the close coupling of heterotrophic bacterioplankton and autotrophs. Here we investigated the responses of a heterotrophic bacterioplankton assemblage to high pCO_2 (790-ppm) treatment in warm tropical western Pacific waters by conducting a microcosm experiment in dark for 12 days. Heterotrophic bacterioplankton abundance and production were enhanced by OA over the first 6 days of incubation, while the diversity and species richness were negatively affected. Bacterioplankton community composition in the high pCO_2 treatment changed faster than that in the control. The molecular ecological network analysis showed that the elevated CO_2 changed the overall connections among the bacterial community and resulted in a simple network under high CO_2 condition. Species-specific responses to OA were observed and could be attributed to the different life strategies and to the ability of a given species to adapt to environmental conditions. In addition, high-throughput functional gene array analysis revealed that genes related to carbon and nitrogen cycling were positively affected by acidification. Together, our findings suggest that OA has direct effects on heterotrophic bacterioplankton in a low-latitude warm ocean and may therefore affect global biogeochemical cycles.

1 Introduction

Increasing greenhouse gases, such as carbon dioxide (CO_2), in the atmosphere are thought to cause global warming and climate change (Cox et al., 2000; Joos et al., 1999; Shakun et al., 2012). The concentration of atmospheric CO_2 is regulated in large part by the ocean, which acts as a huge carbon reservoir. It has been suggested that the global oceans have absorbed approximately 25% of anthropogenic CO_2 emissions over the last decade (2006–2015; Le Quéré et al., 2016) and therefore reduces global warming (Cox et al., 2000; Raven et al., 2005). CO_2 readily reacts with seawater, and the carbon is stored as soluble ions, such as CO_3^{-} (Maier-Reimer & Hasselmann, 1987). The increase in dissolved CO_2 in the global ocean reduces the pH of seawater and results in ocean acidification (OA). Long-term time series observations and ship-based surveys have shown a significant increase in pCO_2 and a significant reduction in pH in the upper ocean (Dore et al., 2009; Watson et al., 2009). It is expected that the decrease in pH in the surface of the ocean will be as great as 0.2 to 0.4 units by the end of this century (Caldeira & Wickett, 2003; Stocker, 2014). Over the last decade, relatively extensive laboratory and field investigations of marine primary producers (e.g., Trichodesmium, picoplankton, and diatoms) and calcifying organisms (e.g., corals, molluscs, and coccolithophores) have shown the sensitivity of many ecologically and biogeochemically important organisms to high pCO_2 levels (Beaufort et al., 2011; Hall-Spencer et al., 2008; Hoegh-Guldberg et al., 2007; Hofmann et al., 2010; Hong et al., 2017; Hoppe et al., 2018; Hutchins et al., 2007; Newbold et al., 2012; Riebesell et al., 2007; Rodolfo-Metalpa et al., 2011; Shi et al., 2010; Tatters et al., 2013).

Bacterioplankton are the other ecologically and biogeochemically important organisms in the ocean. In the classic marine food web framework, bacterioplankton utilize 10% to 50% of carbon fixed by phytoplankton (Azam et al., 1983). Part of the utilized carbon is respired by the bacterioplankton (40%–90%), and the remainder is converted to bacterial biomass, which can be transferred either to higher trophic levels by predation or to the marine organic pool by viral lysis (Azam et al., 1983; Azam & Malfatti, 2007; Fuhrman, 1999). Recently, the importance of bacterioplankton in the transformation of labile DOC into refractory DOC was highlighted by Jiao et al. in the microbial carbon pump theory (Jiao et al., 2010). Bacterioplankton are also involved in the nitrogen cycle, and some steps (e.g., anammox and ammonia oxidation) are known to be mediated only by bacterioplankton (Arrigo, 2004; Francis et al., 2007). Hence, researchers are becoming increasingly concerned about the response of bacterioplankton to OA.

Previous microcosm/mesocosm experiments that investigated the responses of bacterioplankton to OA have shown conflicting results (Crawfurd et al., 2017; Grossart et al., 2006; Joint et al., 2010; Newbold et al., 2012; Piontek et al., 2013; Ray et al., 2012; Zhang et al., 2013). One possible explanation is the close coupling between bacterioplankton and phytoplankton (Allgaier et al., 2008; De Kluijver et al., 2010; Hornick et al., 2017; Piontek et al., 2013). The response of autotrophic phytoplankton to OA affects heterotrophic

bacterioplankton and masks the direct impact of OA on heterotrophic bacterioplankton. In a perspective paper, Joint et al. (2010) concluded that marine microbes possess the flexibility to accommodate pH change and that major marine biogeochemical processes other than calcification will not be fundamentally different under future lower pH condition. However, recent studies showed evidences that heterotrophic marine microorganisms can be affected directly by OA (Liu et al., 2010; Weinbauer et al., 2011), such as their hydrolytic enzyme activities (Yamada & Suzumura, 2010) and extracellular glucosidase activity (Piontek et al., 2010). Hence, a key hypothesis we test in this study is that OA will affect heterotrophic bacterioplankton activity, abundance, community diversity, and functional potential in the oligotrophic water without presence of phytoplankton. Therefore, we carried out a microcosm experiment in the oligotrophic western Pacific Ocean to assess the direct influence of OA. The possibility of the masking effects of phytoplankton was reduced by the selection of low-Chl *a* waters, night sampling, and dark incubation. In addition, since the western Pacific Ocean is a part of the *warm pool*, having annual sea surface temperatures above 28 °C, our study developed an experimental scenario with a higher pCO_2 level and a higher temperature, which will provide a better understanding of the response of bacterioplankton, as well as their ecological and biogeochemical roles, to OA and global warming.

2 Materials and Methods

2.1 Experimental Setup

The present study was conducted at station N8-2 (8°N, 128°E) during the western Pacific Warm Pool (WPWP) NSFC opening cruise (Figure S1 in the supporting information). Approximately 1,000 L of seawater were sampled from the surface at night using a submersible pump and was divided equally into four microcosms (polyethylene bags, acid cleaned with 10% HCl). Two microcosms were pumped with 790-ppm CO_2 (high CO_2 treatment), and the other two were pumped with air (set as the control). The 790-ppm CO_2 treatment was prepared by mixing air and pure CO_2 under the automatic control of a continuous CO_2-sensing and controlling system equipped with a CO_2 chamber (CE100-C, Wuhan RUIHUA, China). The high CO_2 and control air were delivered to the microcosms' bottom at a flow rate of approximately 1 L/min and dispersed by a plastic air stone. The temperature was maintained at approximately 29 °C by a circulating water temperature control system. All of the microcosms were incubated for 12 days in the dark. Subsamples were collected every 2 days, except those for the flow cytometer analysis, which were collected each day.

2.2 Environmental Data Collection

The measurement of NH_4^+ was conducted using a shipboard fluorometric flow analyzer (FIA-lab, USA). Samples for other nutrient analysis (NO_3^-, NO_2^-, and dissolved P) were stored in −20 °C until measured using an Auto Analysis III, AA3 instrument (Bran-Luebbe, Germany). The pH, dissolved

oxygen (DO), salinity, and temperature were measured using YSI pH meter (YSI, USA).

2.3 Bacterioplankton Abundance (BA)

Samples for enumeration of bacterioplankton cell number were analyzed by a Becton-Dickson FACSCalibur flow cytometer (Becton Dickinson, San Jose, CA, USA). A 1-mL water sample was stained with 0.01% SYBR Green I in the dark at 37 °C for 30 min (Marie et al., 1997). Yellowish-green fluorescent beads (1 μm) were added as an internal standard. The samples were analyzed at a flow rate of 0.25 μL/s for 1 min. The flowcytometric data were analyzed using WinMDI software 2.9 (Joseph Trotter, Scripps Research Institute, La Jolla, CA, USA).

2.4 Heterotrophic Bacterial Production (BP)

Heterotrophic bacterial production was measured following the protocol described by Kirchman et al. (1985). Briefly, triplicate 10-mL water samples (prefiltered through a 3.0-μm PC membrane) and one control (fixed with 5% trichloroacetic acid (TCA; final concentration) each received 10 nM of ^{3}H-Leucine (specific activity: 80 Ci mmol $^{-1}$, Amersham, UK) and were incubated in the dark for 2 hr at ambient temperature. Then, the samples were fixed by adding 1-mL 50% TCA and filtered onto 0.2-μm pore size cellulose nitrate Millipore (Millipore, Bedford, MA, USA) membrane filters. The filters were washed twice with 3-mL 5% TCA and twice with 2 mL 80% ethanol and transferred to scintillation vials. The incorporated ^{3}H in each sample was determined using a Perkin-Elmer Wallac 1414 scintillation counter (Perkin Elmer Wallac GmbH, Freiburg, Germany). The cell-specific heterotrophic bacterial production was calculated from the BP/BA ratio.

2.5 DNA Extraction, PCR, Pyrosequencing, and Data Analysis

For DNA extraction, 1 L of seawater from each microcosm was prefiltered through a 3.0-μm (47-mm) PC membrane (PALL Corporation, New York, USA) and then filtered onto a 0.22-μm (47-mm) PC membrane. The total genomic DNA of the filtered water samples was extracted using an Omega Water DNA extraction kit (Omega Bio-Tek, Doraville, CA) from the 0.22-μm (47-mm) PC membrane and eluted in 50-μL TE buffer (10-mM Tris-HCl and 1-mM EDTA, pH = 8.0) following the manufacturer's instructions.

For pyrosequencing, the V3 and V4 regions of 16S rRNA were amplified using the barcoded primers 341F (5′-adaptor + barcode + CCTAYGGGRBGCASCAG-3′) and 806R (5′-adaptor + GGACTACNNGGGTATCTAAT-3′; Beman et al., 2007). The PCR reaction was performed in a 25-μL reaction volume containing 1.5-mM $MgCl_2$, 1× PCR buffer, 0.5 μM of each primer, 0.2 mM of each dNTP, 1.0 unit of Platinum® Taq DNA Polymerase (Invitrogen, Shanghai, China) and 1-μL template DNA. The PCR was performed under the following conditions, 5-min initial denaturation at 95 °C followed by 30 cycles of 95 °C for 30 s, 55 °C for 30 s, and 72 °C for 60 s, and then a final extension at 72 °C for 7 min before holding at 4 °C. All of reactions were

performed in triplicate. The PCR products were gel-purified using a QIAquick gel purification kit (Qiagen, Hilden, Germany) and sequenced by the South Gene Company (Shanghai, China) using Roche 454 GS FLX/+ Platform.

Analysis of the 16S rRNA gene data was conducted using the microbial ecology community software program Mothur (Schloss et al., 2009) following the Schloss standard operating procedure (http://www.mothur.org/wiki/454_SOP). Briefly, the reads were processed by removing tags and primers, accepting only reads with an average quality score above 20 and read lengths between 300 and 500 nt, and removing chimaeras. Denoising was carried out using the command *shhh.seqs* with a sigma value of 0.01. Sequences were classified using the Greengenes database (http://greengenes.lbl.gov/cgi-bin/nph-index.cgi) with a cutoff of 60%. Then, the sequences affiliated with the chloroplast and mitochondria were removed. The numbers of operational taxonomic units (OTUs) were calculated with a cutoff level of 97% nucleotide identity. OTUs containing 1 sequence were removed, and finally, 3,873 sequences were subsampled from each sample. The sample coverage, Chao1 richness estimator, and Shannon diversity index were calculated at a level of 97% similarity. A nonmetric multidimensional scaling (NMDS) analysis was applied using the R-package vegan (Oksanen et al., 2007) to compare the community composition based on the relative abundance of OTUs. OTUs were also classified using the Greengenes database with a cutoff of 60%. The relative abundance of the 15 most abundant heterotrophic bacterial families, accounting for >85% of the reads recovered in this study, were square root transformed and used to generate a heat map using Heml (Deng et al., 2014). In order to identify associations between bacterial families, we calculated the maximal information coefficient (MICe) between bacterial families using MICtools (Albanese et al., 2018; Reshef et al., 2016). Statistically significant co-occurrence relationships ($p < 0.01$) between pairs of variables were input into Cytoscape v 2.8 (Shannon et al., 2003). To determine significant differences between bacterial communities in the control and high CO_2 treatments, the Statistical Analysis of Metagenomic Profiles (STAMP) software package was used (Parks et al., 2014). A table of the relative abundance of each family was used as input. *P* values were calculated using a two-sided *t* test.

To understand the interactions among the bacterial OTUs under different pCO_2 levels, we employed a molecular ecological network (MEN) method (Deng et al., 2012). In order to form a reliable correlation and comparable MENs between control and treatment, only OTUs found at least in 7 of 13 samples in each control and treatment were selected for network construction. The MENs construction was conducted in MENAP (http://ieg2.ou.edu/MENA; Deng et al., 2012). The relative abundance of OTUs was log-transformed, and missing values were filled with 0.01 if paired valid values were available. Similarity matrices (adjacency matrix) were created for each network based on the pairwise Pearson correlation

coefficient across the time series (two-time points lag). The threshold of pairwise Pearson correlation coefficient values between OTUs was identified by a random matrix theory-based approach that observed a transition point of nearest-neighbor spacing distribution of eigenvalues from Gaussian to Poisson distribution (Zhou et al., 2010). Then, a same cutoff of 0.89 was obtained to construct the microbial community networks. Additionally, ecological networks predicted by R^2 ($R^2 > 0.8$) generated based on the random matrix theory should be scale free (Zhou et al., 2010). Once the MEN was determined, the topological indices were calculated based on the adjacency matrix. Module detection of each network was based on fast greedy modularity optimization (Newman, 2006). Identification of key module members was based on within-module connectivity (Zi) and among-module connectivity (Pi) of each node (Olesen et al., 2007). Networks were visualized by the Cytoscape 3.6.1 (Assenov et al., 2008).

All sequences obtained in this study have been deposited in the National Center for Biotechnology Information Sequence Read Archive under the accession numbers SRR6318695 and SRR6318719.

2.6 GeoChip Hybridization and Data Analysis

The labeling and hybridization of extracted DNA followed the method described by (Tu et al., 2014). Briefly, 1-μg genomic DNA from each sample was used for labeling with Cy3 fluorescent dye (GE healthcare) and then hybridized to GeoChip 4 at 42 °C and 40% formamide on Maui hybridization station (BioMicro Systems, Salt Lake City, UT, USA) at 42 °C for 16 hr. The microarrays were scanned using a Nimblegen MS 200 microarray scanner (Nimblegen, Madison, WI) at 100% laser power and photomultiplier tube gain. The signal intensities of each spot were extracted using the NimbleScan software (Nimblegen). Spots with a signal-to-noise ratio greater than 2 were considered to be positive signals.

The GeoChip data were normalized for further analysis by the following steps: (i) removing genes detected in only one of two replicates, (ii) normalizing the signal intensity of each spot by dividing the mean value of each sample by the total signal intensity, and (iii) summing the total signal intensities of each functional gene category. A hierarchical cluster analysis of functional genes was performed using an unweighted pairwise average-linkage clustering algorithm (Eisen et al., 1998). The hierarchical clustering of functional genes was performed and visualized using HemI (Deng et al., 2014).

2.7 Statistical Analyses

The significance of different treatment effects in the incubation was assessed by using the *t* test (each day) and analysis of variance (ANOVA; over the course of the experiment). All statistical analyses were performed using SPSS statistical software (SPSS Inc.).

3 Results

3.1 Environmental Parameters

The pH of the WPWP surface water was 8.3, and it gradually decreased to 8.08 after pumping into high CO_2 air, which was approximate 0.2 unit lower than the control (Figure S2a). DO concentration dropped from around 6.3 to 5.6 mg/L in both control and treatment microcosms in the first 4 days of incubation and then increased to 6.3 mg/L at day 6 (Figure S2b). Salinity and temperature were around 35.0 °C and 29 °C, respectively, in all microcosms during incubation. The concentration of NH_4^+, NO_3^-, NO_2^-, and dissolved P were lower than the detection limit (The detection limits for NH_4^+, NO_3^-, NO_2^-, and dissolved P were 0.5, 0.1, 0.04, and 0.08 μmol L^{-1}, respectively).

3.2 Bacterioplankton Abundance

The abundance of picophytoplankton and bacterioplankton (BA) was 1.21×10^5 and 6.18×10^5 cells mL^{-1} at the start of incubation, respectively. Two heterotrophic bacterioplankton growth phases, bloom (high CO_2treatment: days 0–6; control: days 0–8) and postbloom (high CO_2 treatment: days 6–8; control: days 8–10), were observed during incubation (Figure 1). BA in the control and the high CO_2 treatment gradually increased during the bloom phase and peaked at day 8 ($1.80 \times 10^6 \pm 1.85 \times 10^5$ cells mL^{-1}) and day 6 ($2.15 \times 10^6 \pm 9.30 \times 10^4$ cells mL^{-1}), respectively (Figure 1a). The bloom peak in the high CO_2treatment microcosms was significantly higher than that in the control (Chi-square analysis: $df = 1$, $p < 0.01$). The abundance of picophytoplankton decreased quickly to an undetectable level after 2-days incubation.

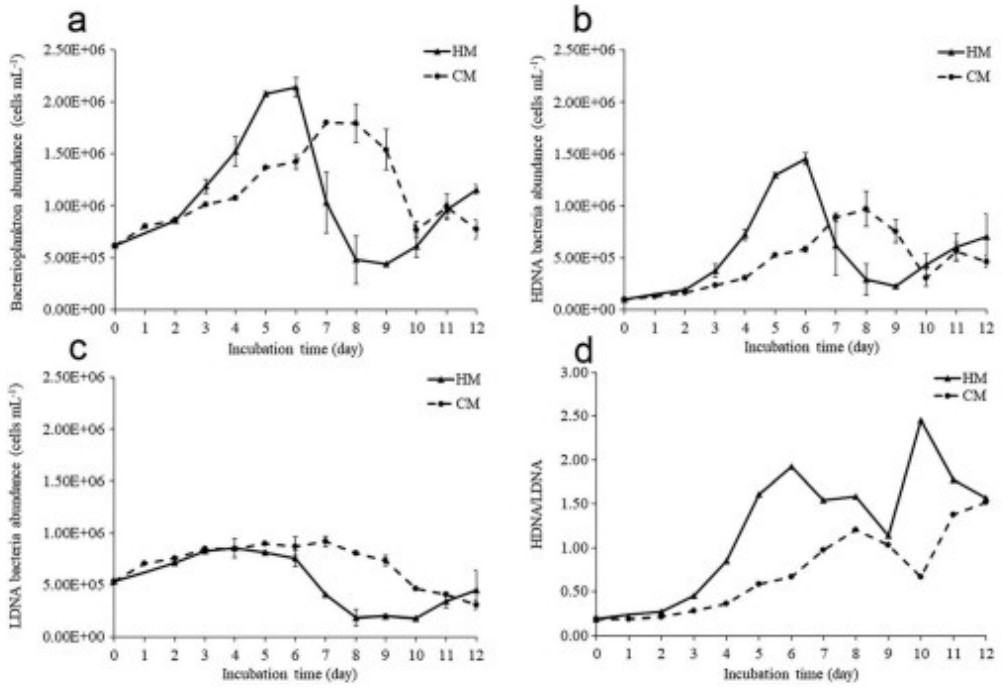

Figure 1. Bacterioplankton abundance over time. (a) Bacterioplankton. (b) High DNA bacteria. (c) Low DNA bacteria. (d) The ratio of HDNA bacteria/LDNA bacteria. HM: high CO_2 microcosm. CM: control microcosm. The day 1 samples from the HMs were lost.

We further resolved the bacterioplankton community into high (HDNA) and low (LDNA) nucleic acid groups based on fluorescence intensity and light scatter properties according to protocol of Lebaron et al. (2002). The abundance of LDNA bacterioplankton in the in situ surface water of the WPWP was 5.32×10^5 cells mL^{-1}, which was approximately 5 times higher than that of the HDNA bacterioplankton (day 0; Figures 1b and 1c). The HDNA bacterioplankton showed a markedly higher growth rate than the LDNA bacterioplankton during the bloom phase (ANOVA, $p < 0.05$), and the growth of the HDNA bacterioplankton could be enhanced by OA. However, during the postbloom phase, both the HDNA and LDNA bacterioplankton in all the microcosms decreased quickly, and the latter displayed a higher mortality rate in the high CO_2 treatment than in the control (Figure 1c). The HDNA/LDNA ratio gradually increased during 12 days of incubation and was generally higher in the high CO_2 microcosms than in the control (Figure 1d).

3.3 Heterotrophic Bacterial Production

The heterotrophic bacterial production (BP) in all the microcosms increased rapidly during the heterotrophic bloom phase (Figure 2). The highest BP reached 10.52 ± 0.33 μg C L^{-1} h^{-1} in the high CO_2treatment at day 4 and 10.10 ± 0.16 μg C L^{-1} h^{-1} in the control at day 8. Over the first 4 days of incubation, the BP was significantly higher in HM than in CM (*t* test, $p < 0.05$), suggesting that it was positively affected by acidification (Figure 2a) during the bloom phase. However, in the postbloom phase, although BA

decreased in all the microcosms, no obvious decrease in BP was observed. The cell-specific heterotrophic bacterial production continually increased in the control during incubation, while no clear trend was observed in the high CO_2treatment (Figure 2b). Generally, the cell-specific heterotrophic bacterial production was higher in the high CO_2treatment than in the control.

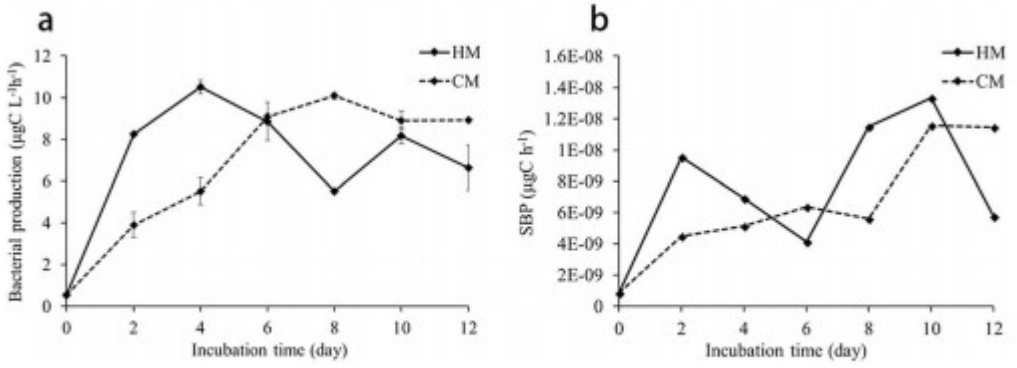

Figure 2. The response of heterotrophic bacterioplankton production to ocean acidification. (a) Heterotrophic bacterial production. (b) Cell-specific bacterial production. HM: high CO_2 microcosm. CM: control microcosm.

3.4 Bacterioplankton Community Composition

In total, 357,392 16S rRNA gene sequences were obtained by 454 pyrosequencing. After the low-quality sequences were removed, 3,873 reads were subsampled from each sample, and these reads were clustered into 505 OTUs with a 97% sequence similarity threshold. The number of OTUs ranged from 157 to 414 across all the samples. The sequences statistic can be found in Table S1. Although the rarefaction curves did not reach plateau, coverage of most samples were higher than 95% (Figure S3), indicating subsample of 3,873 sequences could cover most of bacterial taxonomic diversity (Table S1 and Figure S3). The bacterial species richness decreased from 41 to 30 in CM and from 41 to 26 in HM over the incubation period (Figure 3). OA resulted in a lower species richness (day 2 to day 10), and the highest difference in richness was observed during the bloom phase. Similarly, the Shannon diversity index, which indicates the diversity of the bacterioplankton community, was also significantly negatively affected by OA from day 4 to day 12 (ANOVA, $p < 0.05$). The bacterioplankton community displayed low richness and diversity when the BA reached its highest value in the high CO_2treatment (day 6) and in the control (day 8; Figure 3). The richness and diversity in the high CO_2 treatment at day 6 were significantly lower than that in the control at day 8 ($p < 0.05$; Figure 3).

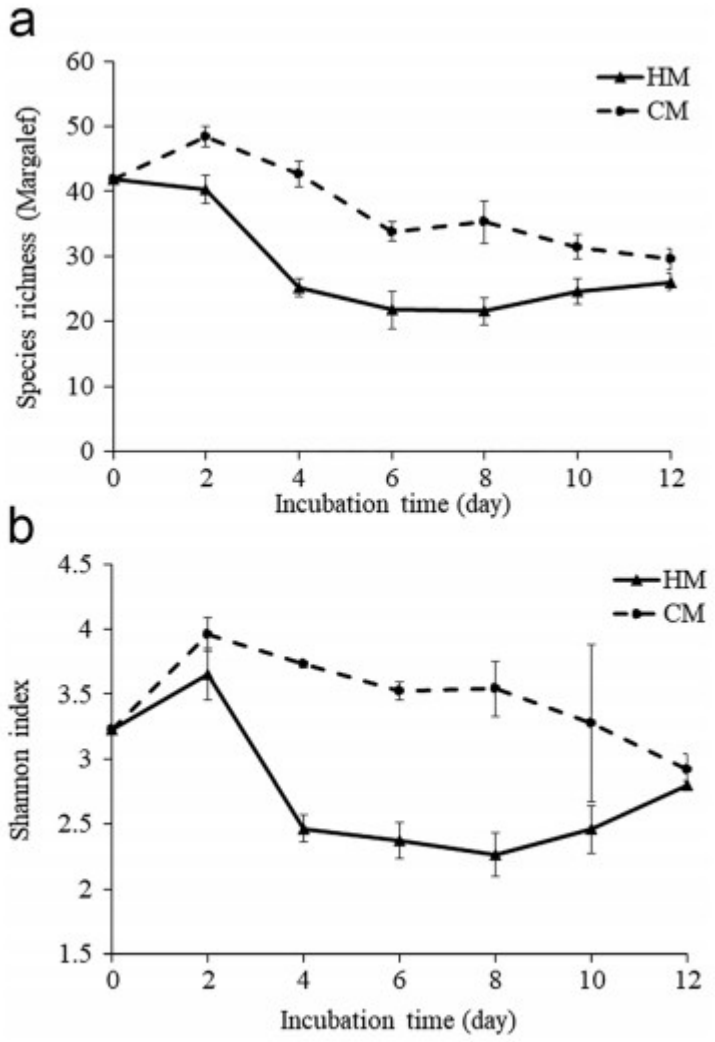

Figure 3. Bacterial community species richness (a) and diversity (b) over time. HM: high CO_2 microcosm. CM: control microcosm. Errors bars represent SD of replicate samples.

NMDS analysis showed a temporal variation in bacterioplankton community composition in the microcosms (Figure 4). A daily increase in the dissimilarity between the initial and incubation communities was recorded. The bacterioplankton community composition in the high CO_2treatment changed faster than that in the control (Figure 4). The control treatment and high CO_2 treatment had distinct community compositions during the bloom phase (e.g., high CO_2treatment: days 0–6; control treatment: days 0–8).

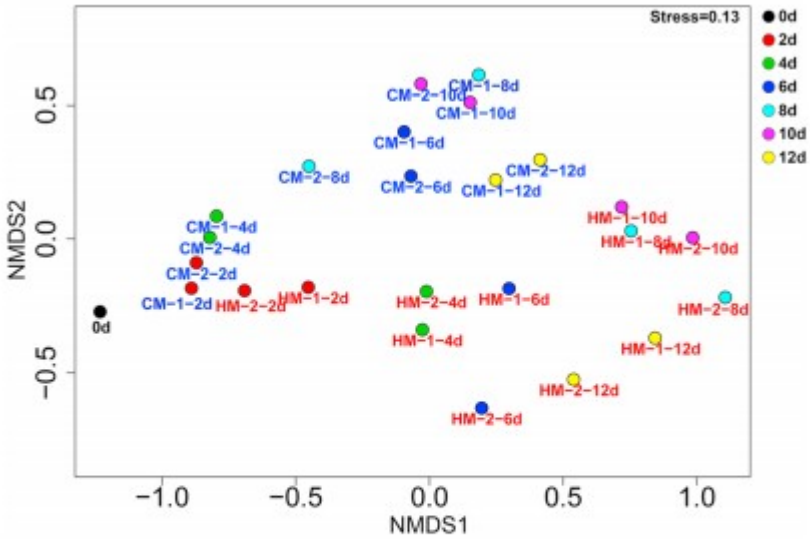

Figure 4. NMDS analysis showing the relationships between the bacterioplankton communities in the high CO_2treatment (indicated in red text label) and the control (indicated in green text label) during 12 days of incubation. HM: high CO_2 microcosm. CM: control microcosm.

Based on the Greengenes database (60% threshold), all the sequences were assigned to 26 bacterial phyla. Proteobacteria (58.3%) was the most common phylum in the WPWP, followed by Cyanobacteria (26.8%), Bacteroidetes (6.5%), Actinobacteria (3.1%), SAR406 (1.7%), and Planctomycetes (1.5%; Figure S4, day 0). The relative abundance of Cyanobacteria decreased from 26.8% to less than 3.0% in all the microcosms after 12 days of incubation, suggesting that the growth of phytoplankton was inhibited by light limitation (Figures S4 and S5). To focus on the impact of OA on heterotrophic bacteria, Cyanobacteria were not included in the subsequent analyses.

The bacterial phyla showed different responses to the increase in pCO_2 (Figures S4 and S5). The relative abundance of Proteobacteria in both the high CO_2treatment and the control increased from 57.8% to more than 90% after 6 days of incubation and was generally higher in the high CO_2 microcosms than in the control (Figure S5). In contrast, Actinobacteria and SAR406 decreased quickly during incubation. From day 2 to day 10, Actinobacteria and Planctomycetes had significantly higher relative abundance in the control, suggesting that they might be negatively related with acidification. Similarly, SAR406 displayed a higher relative abundance in CM from day 2 to day 4. Bacteroidetes, the third most abundant phylum in the WPWP, was relatively more abundant in HM during the bloom phase but more abundant in CM postbloom (Figure S5).

At the family level, Pelagibacteraceae was the most abundant family in the in situ surface water of the WPWP at 37.4% (Figure S6). The relative abundance

of this family, together with that of Halomonadaceae, Flavobacteriaceae, OCS155, AEGEAN_112, A714017, and Pirellulaceae, gradually decreased during incubation. In contrast, Rhodobacteraceae and Hyphomonadaceae increased after incubation (Figure 5). Bacteriovoracaceae and OM27 were more abundant in the postbloom phase. The bacterioplankton families also displayed different responses to OA (Figure 5). For example, Rhodobacteraceae were generally positively affected by OA, and Hyphomonadaceae was enhanced by acidification during the bloom phase. In contrast, Pelagibacteraceae, Halomonadaceae, OM60, Pseudoalteromonadaceae, and Alteromonadaceae were generally negatively affected by acidification (Figure 5).

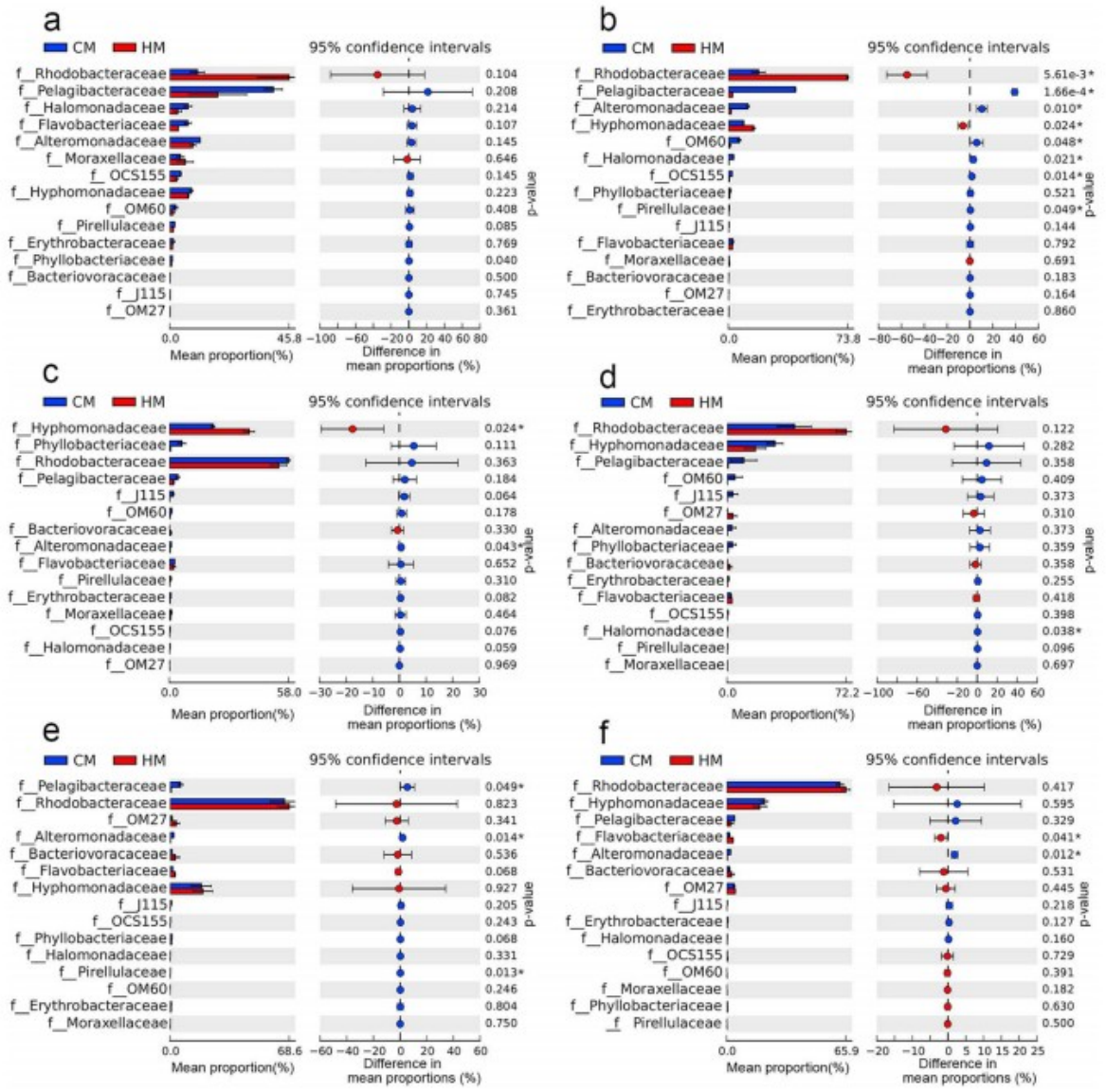

Figure 5. The STAMP (Statistical Analysis of Metagenomic Profiles) analysis of the relative abundance of the heterotrophic bacterioplankton families enriched or depleted between the control (blue) and the high CO_2treatment (red) on days 2 (a), 4 (b), 6 (c), 8 (d), 10 (e), and 12 (f). The groups overrepresented in the control correspond to positive differences between proportions, and the groups overrepresented in the high CO_2treatment correspond to negative differences between proportions. Corrected *p* values were calculated using *t* tests.

The 15 most abundant bacterioplankton families among all samples (covering more than 85% of the total community) were selected to generate correlation patterns. In the network, it is clear that the two most abundant bacterial families, Pelagibacteriaceae and Rhodobacteriaceae, were negatively correlated with each other. As shown in Figure 6a, bacterial families OM60, Alteromonadaceae, J115, Moraxellaceae, OCS155, Halomonadaceae, and Pirellulacae were positively correlated with Pelagibacteraceae (Figure 6). Rhodobacteraceae, which was the most

abundant family and was positively affected by acidification (Figure 5), showed positive correlations with Hyphomonadaceae, OM27, and Bacteriovoracaceae (Figure 6).

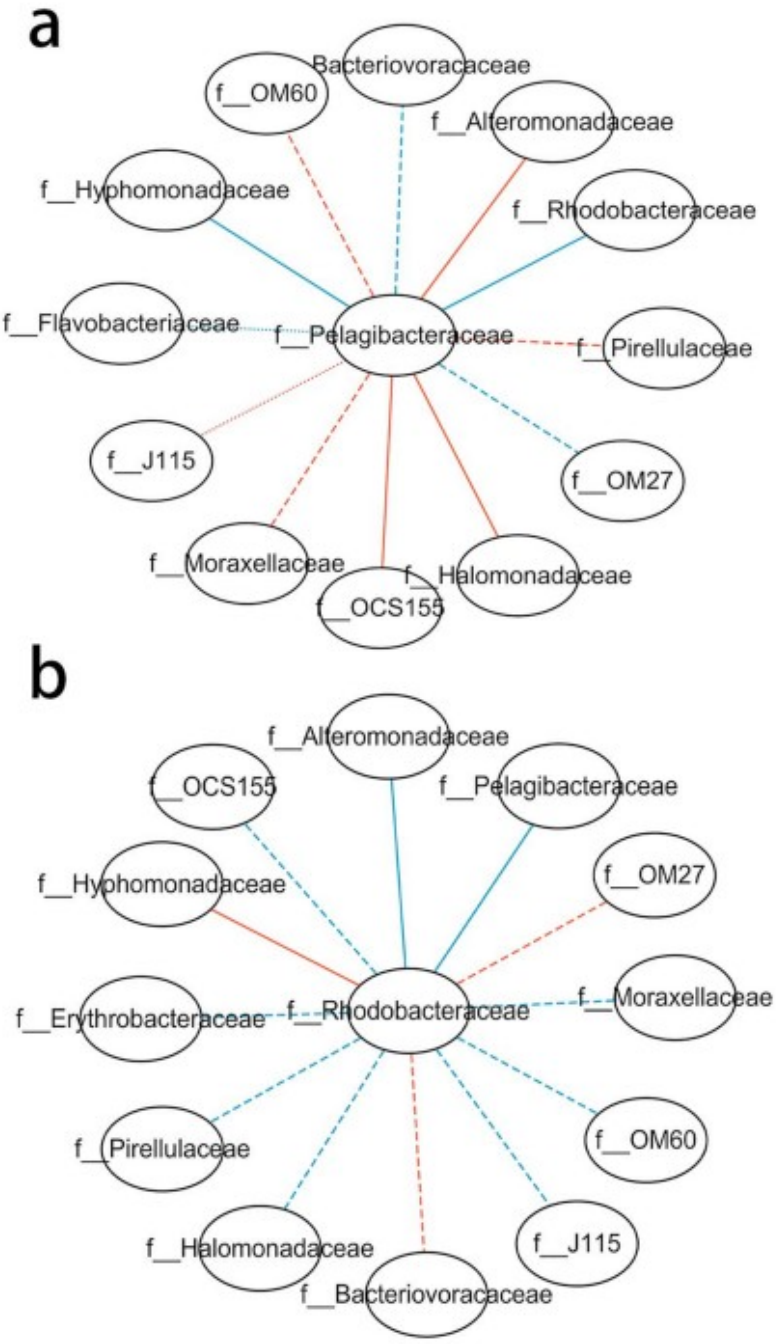

Figure 6. Network analysis demonstrating significant ($P < 0.01$) associations only between (a) Pelagibacteraceae and (b) Rhodobacteraceae and other bacterial families. Positive linear regressions between nodes are denoted by red lines; negative linear regressions are blue lines. MICe ≤ 0.5: dot lines, $0.5 <$ MICe ≤ 0.8: dash lines, $0.8 <$ MICe ≤ 1: solid lines. The matrix used to calculate the MICe correlation was obtained as the average relative abundance of a bacterioplankton family in the high CO_2 microcosms on a specific day minus the average relative abundance of that same family in the control microcosms.

In the WPWP, Pelagibacteraceae were mainly represented by OTU3 (Pelagibacteraceae clade Ia; Figure 7, day 0, and Figure S7). The relative abundance of this OTU gradually decreased during incubation and was higher in the control. Rhodobacteraceae and Hyphomonadaceae, which were positively affected by acidification, were mainly composed of OTU1 and OTU2, respectively (Figure 7). OTU1 was classified as *Rhodovulum* sp., and OTU2 belonged to *Hyphomonas* sp. OTU5, which also had a relatively high abundance in the microcosms, was affiliated with the genus *Nautella* (family Rhodobacteraceae) and was more abundant in the high CO_2treatment.

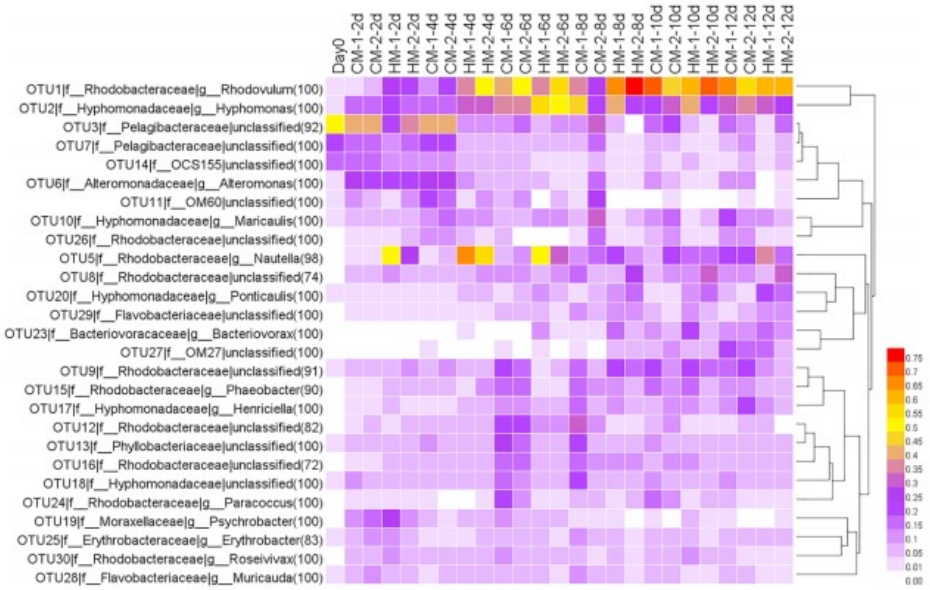

Figure 7. Heatmap showing the relative abundance of the top 30 abundant OTUs in the high CO_2 treatment and the control during incubation (two unclassified families and a Cyanobacteria OTU were not included).

The molecular ecological network (MEN) analysis showed that 104 and 63 nodes were identified from the elevated CO_2 network and control network respectively, while 313 and 93 links were found separately (Table 1 and Figure 8). The more complex ecological network in the control than in the elevated CO_2 treatment may be a consequence of the higher bacterial richness. Several overall network topological indices were calculated, including average connectivity (avgK), average clustering coefficient (avgCC), and average geodesic distance (avgGD; Table 1). The values of the avgK and avgGD were greater in the control microcosm, while the avgCC and modularity were greater in the high CO_2 microcosm. These results suggested that the elevated CO_2 changed the overall connections among the bacterial community and resulted in a simple network.

Table 1
Major Properties of Molecular Ecological Network

	# nodes	# links	R^2 of power law	avgK[a]	avgCC	avgGD
Control	104	313	0.873	6.019	0.21	3.364
Treatment	63	93	0.899	2.952	0.22	3.331

[a]avgK: average connectivity; avgCC, average clustering coefficient; avgGD, average geodesic distance.

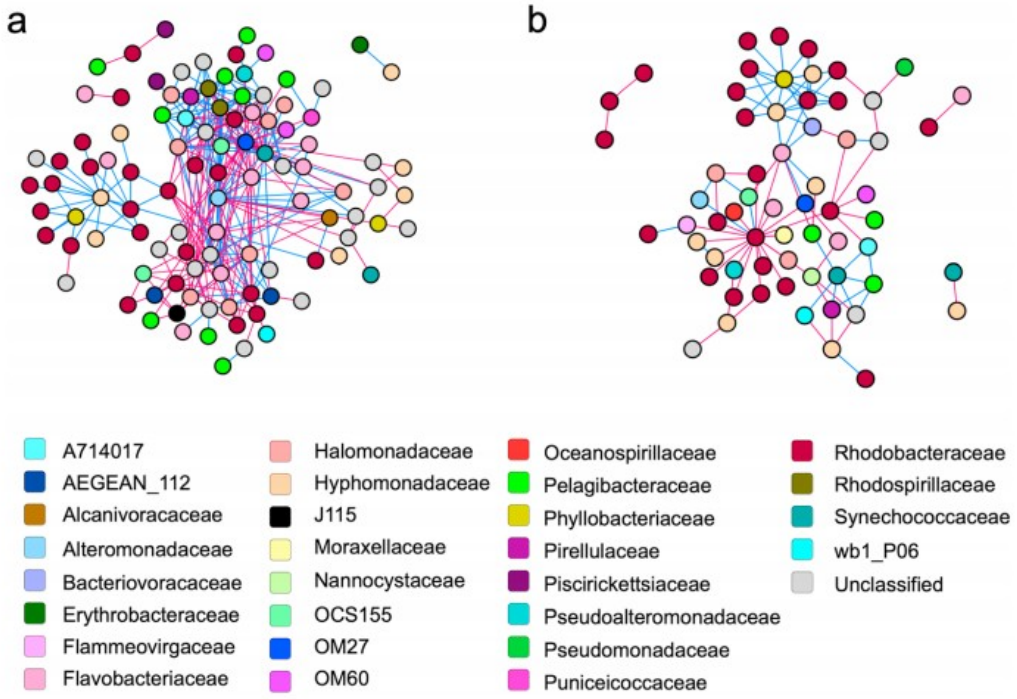

Figure 8. Molecular ecological network of control (a) and elevated CO_2 (b) mesocosm. Each node indicates an OTU, where the link between each two nodes indicates the correlation between two OTUs. Colors indicate different bacterial classes. The blue link indicates the positive correlation, while red link indicates the negative correlation.

The Flavobacteriaceae, Hyphomonadaceae, Pelagibacteraceae, and Rhodobacteraceae dominated the both treatment and control networks (Figure 8), which indicated their important roles in the microbial communities. The proportion of positive and negative links was similar in both networks separately. In the control, 162 positive links and 151 negative links were observed, while only 46 positive and 47 negative links were found in the treatment.

As showed in Figure 9, OTUs affiliated with Flavobacteriaceae were the network connectors in both control and treatment networks.

Hyphomonadaceae played an important role as module hub in the control microcosm network, while Rhodobacteraceae in the treatment microcosm network. No OTU was shared as module hub and network hub between the two networks.

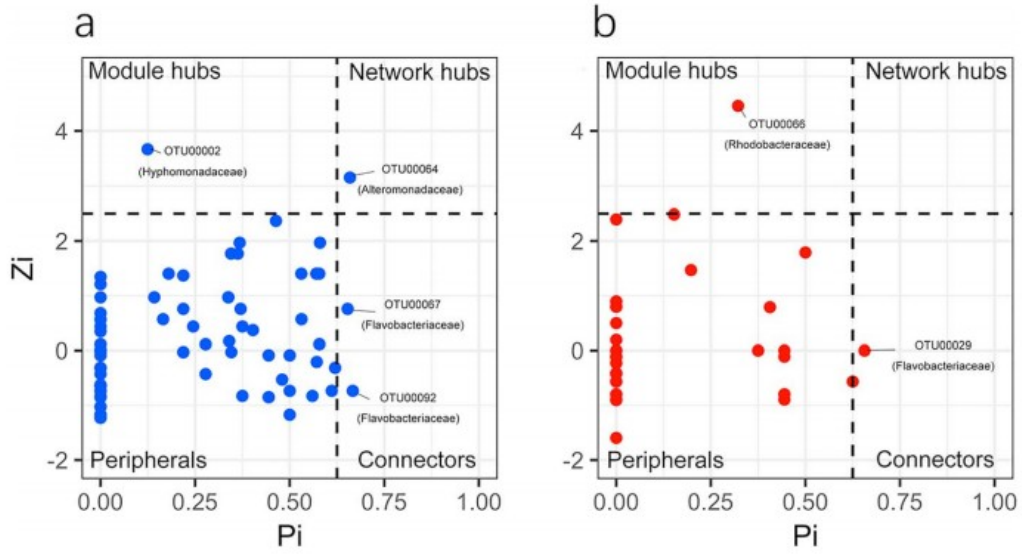

Figure 9. Submodules under control (a) and elevated CO_2 (b) mesocosms. Each node indicates an OTU. The Z-P plot showing OTU distribution based on their module-based topological role according to within-module (Z) and among-module (P) connectivity. The nodes of Zi > 2.5 and Pi <0.625 are indicated as the module hubs that were closely connected within the module, while the nodes of Zi < 2.5 and Pi >0.625 are the connectors that were more closely connected to nodes in other modules. Peripherals of Zi < 2.5 and Pi <0.625 are considered specialists in each module, while the network hubs of Zi > 2.5 and Pi >0.625 are supergeneralists.

3.5 Response of Bacterial Functional Potential to Increased pCO_2

The GeoChip 4 detected a substantial number of functional gene probes across all samples, including genes involved in C and N cycling. To evaluate the influence of elevated CO_2 on the major processes of C cycling, we examined 41 C-cycling-related genes (Figure 10a). Among these genes, 4 were involved in carbon fixation and 34 genes were related to the degradation of complex carbon substrates, such as cellulose, starch, and chitin. We observed that the genes involved in lignin, hemicellulose, chitin, and cellulose degradation were markedly enriched by acidification (ANOVA, $p < 0.05$). Most of the genes related to carbon degradation reached their highest abundance in the high CO_2 microcosms at day 8, when BA was the highest.

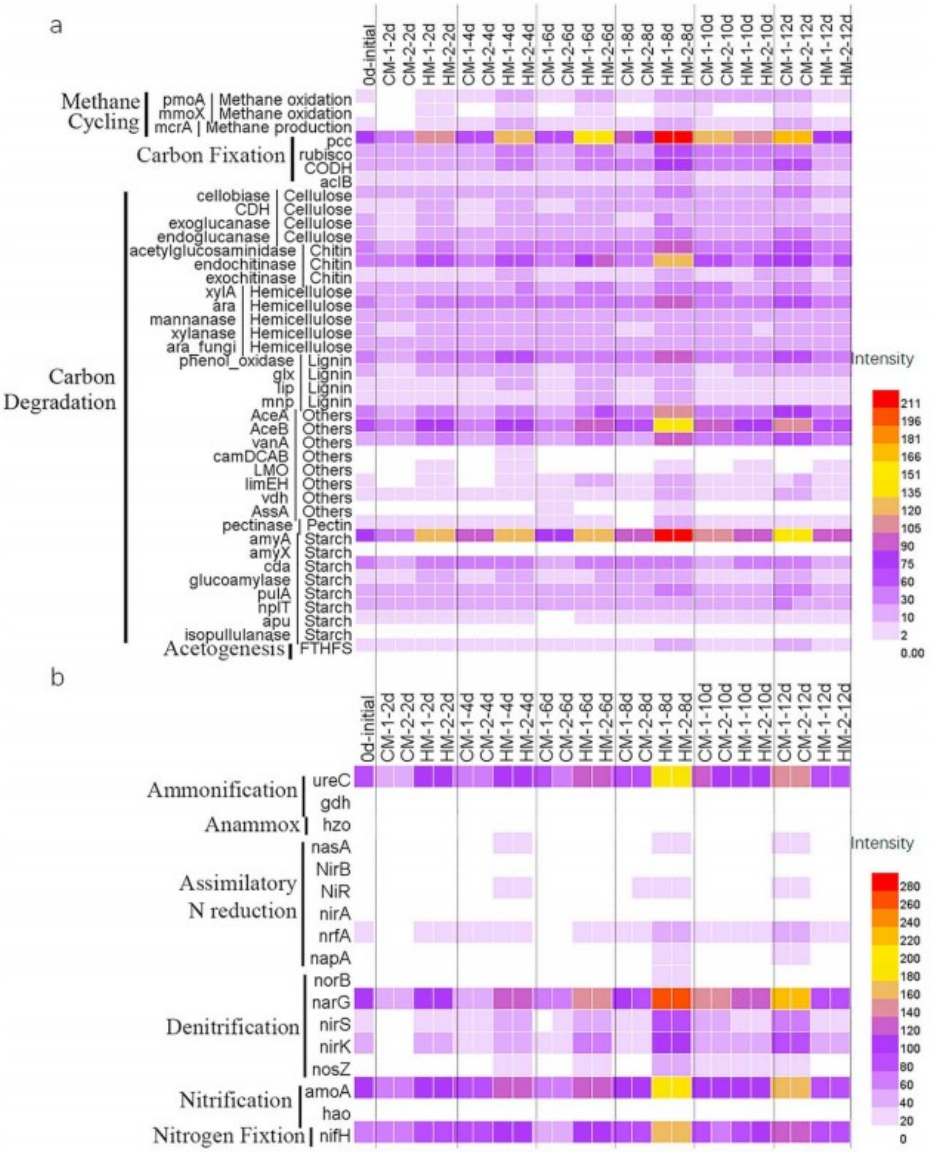

Figure 10. Heatmap showing abundance changes of carbon-cycling-related genes (a) and nitrogen-cycling-related genes (b) to acidification.

We also examined the response of N-cycling-related genes to OA (Figure 10b). Among them, *nifH* (nitrogen fixation), *amoAB* (nitrification), *narG* (denitrification), and *ureC* (ammonification) were abundant in the WPWP (Figure 10b, day 0). The relative abundance of these four genes gradually increased during 12 days of incubation. Over the course of the experiment, the presence of N-cycling-related genes was significantly different in the HM and CM (ANOVA, $p < 0.05$). Generally, all the detected N-cycling genes, with the exception of the *hao* gene, had a higher intensity in the high CO_2 treatment from day 2 to day 8.

4 Discussion

The effects of OA on bacterioplankton have been intensively studied during the last decade. However, most of the previous studies were conducted under light conditions in the presence of autotrophs (e.g., Allgaier et al., 2008; Zhang et al., 2013). The strong response of autotrophic phytoplankton to OA (positive or negative), often exerting a strong effect on the heterotrophic bacterial community and masking direct response of bacterioplankton to OA. For example, due to the presence of different processes of organic matter production and consumption at the same time that is difficult to disentangle, previous studies showed inconsistent results regarding the effect of OA on BA. The mesocosm experiments conducted in Bergen (Grossart et al., 2006) and the Baltic Sea (Lindh et al., 2013) suggested that OA has no or little impact on BA, while studies in the Ross Sea (Maas et al., 2013) and a Norwegian fjord (Galgani et al., 2014) showed that BA can be stimulated by acidification. To overcome this possible bias, we conducted experiments under dark conditions to limit the growth of phytoplankton to better understand how heterotrophic bacterioplankton communities are directly affected by OA (Hornick et al., 2017).

4.1 Acidification Stimulated Bacterioplankton Activity

Increased BP with elevated CO_2 has been reported by previous studies (Endres et al., 2014; Grossart et al., 2006; Piontek et al., 2010). For instance, a study conducted on Antarctic coastal waters during the austral summer found that BP was higher under elevated CO_2 over the first 4 days of incubation (Westwood et al., 2018). It has been suggested that the increases in BP are caused by the increase in phytoplankton-derived DOM under OA. However, another explanation is that the increase in BP under OA may be due to an increase in the activity of bacterial extracellular enzymes, such as glucosidase and lipase (Burrell et al., 2015; Endres et al., 2014; Grossart et al., 2006; Maas et al., 2013; Piontek et al., 2010; Thomas et al., 2016). In the present study, we observed increase of BP during the bloom phase in both treatment and control microcosms. This should be supported by the organic matters released from the die-off of photosynthetic organisms, such as picocyanobacteria, in the first 2 days. However, we observed that the BP and cell-specific BP were higher in the high CO_2 treatment, supporting the hypothesis that OA enhances BP directly by increasing the activity of extracellular enzymes. The higher BP under elevated CO_2 over the first 4 days was accompanied by high BA (Figure 1). This suggests that the growth of heterotrophic bacteria could be positively affected by OA, although top-down control effects, such as protist grazing (Kim et al., 2010) and viral lysis (Carreira et al., 2013; Larsen et al., 2008; Traving et al., 2014), can also be enhanced by elevated CO_2. We further showed that the increased cell abundance was primarily from HDNA bacteria, or high activity bacteria, indicating that OA enhances bacterial population size by stimulating their activity. Moreover, BA in the high CO_2 microcosms peaked 2 days before the control peak, suggesting that increased bacterial community activity may increase the rate of biogeochemical cycling in the ocean. Our results

therefore further supported the conclusion of Sala et al's study that microbial communities in oligotrophic waters are considerably affected by OA (Sala et al., 2015). It is worth pointing out that because OA is an additional stress for some organisms, it might lead to die-off of these organisms and higher organic matter release, which subsequently affected bacterial production and abundance in this study.

4.2 Heterotrophic Bacterioplankton Species Have Different Responses to OA

Studies in the North Sea (Krause et al., 2012) and the San Juan Channel (Siu et al., 2014) have demonstrated that acidification significantly affects bacterioplankton community composition. In addition, study in Bergen showed community structure of free-living bacteria changed with pCO_2 (Allgaier et al., 2008). On the contrast, some other studies showed that OA has no or little impacts on the bacterioplankton community, such as studies in the Baltic Sea (Lindh et al., 2013) and the Arctic Ocean (Roy et al., 2013; Wang et al., 2015; Zhang et al., 2013). Our new data showed that in low-latitude, oligotrophic warm waters, when the growth of phytoplankton was suppressed, the bacterioplankton community could be significantly affected by acidification in the early phases of incubation (first 6 days), while acidification had little effect in nutrient depleted conditions (postbloom). Other studies have also observed that changes to bacterial community composition after acidification may be linked to nutrient conditions (Bunse et al., 2016; Celussi et al., 2017; Hornick et al., 2017). We observed relatively low bacterial diversity (Figure 3) and relatively simple network of microbial community (Figure 8) under high CO_2 compared to the control microcosm. These results suggested the elevated CO_2 simplified the microbial communities. Similarly, a mesocosm study conducted in the Ross Sea also observed a decrease in bacterioplankton diversity in response to elevated CO_2 (Maas et al., 2013). However, the authors suggested that the loss of diversity did not affect bacterial activity but rather enhanced the ability of the bacterioplankton to break down carbohydrates and lipids and recycle phosphate.

Bacterioplankton species had different responses to acidification (Figures 6 and 7). Of top 20 most abundant families, the *high nutrient loving* bacteria in Rhodobacteraceae (Azam & Malfatti, 2007), primarily *Rhodovulum* and *Nautella*, and Hyphomonadaceae, primarily *Hyphomonas*, remained at a relatively high abundance during the incubation period. This indicates certainorganic matters released from mortality of phytoplankton during the bacterioplankton bloom phase benefitted these families. Earlier studies also observed a higher abundance of Rhodobacteraceae under high CO_2 conditions (Meron et al., 2011; Siu et al., 2014), although another laboratory study of the Rhodobacteraceae strain *Roseobacteria* MED165m showed that elevated CO_2 did not significantly affect its abundance but did increase the growth efficiency of the strain (Teira et al., 2012). These results suggest that different responses to pH could occur at the genus or species level in this highly diverse family, so studying the response of bacteria at the species or

even ecotype level could provide more useful information. The response of Rhodobacteraceae to OA was different during and after the bloom phase, indicating that the influence of OA on this family was dependent on environmental conditions. In the early phase, the availability of bacterial substrates was sufficient, while it was deficient during the postbloom phase. This could partially explain the inconsistent results found in previous studies (Baltar et al., 2015; Krause et al., 2012; Meron et al., 2011; Newbold et al., 2012; Witt et al., 2011). Similar to Rhodobacteraceae, Hyphomonadaceae was not abundant at the start of the experiment but became a major family after incubation. Network analysis showed Hyphomonadaceae, as well as Alteromonadaceae, played important roles in the microbial community in the control microcosm but disappeared in the high CO_2 microcosm (Figure 9), which indicated that they might be sensitive to the OA.

In the current study, we observed a decrease in the relative abundance of Pelagibacteraceae, the most abundant bacterioplankton in the western Pacific Ocean, during incubation, which may due to the lack of light and change of organic matter availability. In our system, the available nitrogen-containing DOC, a major carbon source for Pelagibacteraceae (Jiao & Zheng, 2011), may have been consumed at the beginning of the incubation or the lack of light may have limited the growth of Pelagibacteraceae, since light is needed for uptake of organic nutrients (Gómez-Pereira et al., 2013). Our study showed that Pelagibacteraceae might be negatively affected by acidification. In contrast, a recent high-latitude open ocean study that found that Pelagibacteraceae were not affected by acidification (Hartmann et al., 2016) and another study reported increased levels of Pelagibacteraceae at the end of incubation (Newbold et al., 2012). These inconsistencies may be due to the presence of different phylogenetic groups (Brown et al., 2012). Pelagibacteraceae is composed of more than seven clades, each of which has different physiological characteristics (Grote et al., 2012).

4.3 Biogeochemical Cycles Mediated by Bacterioplankton May Be Changed by Ocean Acidification

Bacteria play key roles in almost all of Earth's biogeochemical cycles. Studying the response of bacterial functional genes to ocean acidification will help us predict the future change in biogeochemical cycles. The global ocean is a large carbon pool, and researchers have proposed the microbial carbon pump as a conceptual framework to depict the generation of this large carbon reservoir (Jiao et al., 2010). In this conceptual framework, marine bacterioplankton are essential for the transformation of organic carbon from labile into recalcitrant states. However, we know little about how ocean acidification will affect organic matter degradation in marine environments. In the present study, we observed that genes involved in polysaccharide (cellulose, chitin, hemicellulose, lignin, and starch) degradation, such as genes encoding endochitinase, were more abundance under OA condition. These types of organic matter are recognized as important components of refractory dissolved organic carbon (DOC) in the ocean (Jiao et al., 2010).

Polysaccharides account for up to 32% of DOC (Pakulski & Benner, 1994) and more than 50% of the total phytoplankton primary production (Baines & Pace, 1991). It has been suggested that acceleration of the degradation of polysaccharides and organic carbon in the global ocean may affect vertical carbon export as these compounds are major components of the sinking particles (Engel et al., 2004; Piontek et al., 2010). Moreover, enhanced degradation of these types of complex organic matter may change the composition of the carbon pool and increase the respiratory production of CO_2. Both an increase in carbon degradation and a decrease in carbon sinking under OA may reduce the ocean's ability to absorb CO_2 from the atmosphere.

Nitrogen fixation conducted by marine microorganisms has a critical role in supporting oceanic new production (Karl et al., 1997; Montoya et al., 2004). Previous studies suggested that the rates of growth and nitrogen fixation of the cyanobacterium *Trichodesmium*, an important diazotroph in oligotrophic oceans, could be positively affected by acidification when Fe and P are not limited, due to the reallocation of energy and resources from carbon-concentrating mechanisms (Levitan et al., 2007). In addition, *Nodularia*, another diazotroph cyanobacteria, showed similar responses to acidification (Wannicke et al., 2012). Our study, which focused on heterotrophic bacteria, showed that the abundance of heterotrophic diazotroph could be enhanced by acidification. Similar results were observed by Rees et al. (2017) who conducted a mesocosm experiment in the coastal western Mediterranean Sea. The significance of heterotrophic diazotroph, such as Gammaproteobacteria, was reported in recent years (Messer et al., 2016; Moisander et al., 2017). They were frequently detected in the global oceans at both DNA and RNA levels. The increase in heterotrophic diazotroph abundance under ocean acidification may enhance inputs of new N and increase primary productivity in future oceans.

Under OA conditions, the genes involved in denitrification and nitrification (mainly *amoA*gene) were significantly increased in the western Pacific Ocean, except for the *hao* gene, which is involved only in nitrification (Figure 10). An increase in the denitrification rate and a decrease of microbial nitrification rates with OA has been reported and suggested a nitrogen cycle *bottleneck* (Hutchins et al., 2009). Similarly, Bemen et al. observed that microbial nitrification rates decreased when pH was experimentally reduced (by 0.05–0.14) in the Atlantic and Pacific Oceans and suggested that ocean acidification could reduce nitrification rates by 3%–44% within the next few decades (Beman et al., 2011). A possible explanation for the inconsistent results observed in this and previous studies is that we conducted incubation under dark conditions, which protected some ammonia oxidizing bacteria and archaea from light inhibition (Merbt et al., 2012; Qin et al., 2014). OA may also cause a change in the diversity of the nitrifier community. Bowen et al. reported that microbial groups capable of ammonia oxidization have different responses to acidification. Some ammonia oxidization bacteria are

significantly influenced by ocean acidification, but not AOA (Bowen et al., 2013). A similar result was also reported by Tait et al. (2014) who found that ammonia oxidizing bacteria and archaea in marine sediments have different pH optima.

5 Conclusions

Generally, this study, conducted in the western Pacific Warm Pool, could provide insights into the impacts of OA on bacterioplankton in oligotrophic warm waters. Our study demonstrated that OA has direct effects on abundance, activity, diversity, community structure, and interaction of heterotrophic bacterioplankton in the low-latitude warm ocean. An increase in genes involved in carbon degradation and fixation in high CO_2 conditions may accelerate carbon turnover. In addition, our results suggest that the response of the bacterioplankton community to OA is related to the pool of bacterial groups within the community and to nutrient conditions. Thus, to reveal the effects of acidification on the bacterioplankton community in the global ocean, further experiments are needed in different geographic locations.

Acknowledgments

This work was supported by the National Natural Science Foundation of China (31570172 and 41861144018) and the Public Science and Technology Research Fund Projects for Ocean Research (201505003-3). R. Z. was partially supported by Qingdao National Laboratory for Marine Science and Technology (QNLM2016ORP0303), the Senior User Project of RV KEXUE (KEXUE2018G07), and the Fundamental Research Funds for the Central Universities (20720180123). This work was also supported by the CAS Pioneer Hundred Talents Program and the South China Sea Institute of Oceanography, CAS for the project Different niches of Synechococcus ecotypes (Y8SL031001). All sequences obtained in this study for Figures 3-9 were deposited in https://www.ncbi.nlm.nih.gov/sra under the accession numbers SRR6318695 and SRR6318719. Data for Figures 1 and 2, as well as GeoChip data for generating Figure 10, were included in supporting information Data Sets S1 and S2.

References

Albanese, D., Riccadonna, S., Donati, C., & Franceschi, P. (2018). A practical tool for maximal information coefficient analysis. *GigaScience*, 7(4), 1– 8. https://doi.org/10.1093/gigascience/giy032

Allgaier, M., Riebesell, U., Vogt, M., Thyrhaug, R., & Grossart, H.-P. (2008). Coupling of heterotrophic bacteria to phytoplankton bloom development at different pCO_2 levels: A mesocosm study. *Biogeosciences Discussions*, 5(1), 317– 359. https://doi.org/10.5194/bgd-5-317-2008

Arrigo, K. R. (2004). Marine microorganisms and global nutrient cycles. *Nature*, 437, 349– 355.

Assenov, Y., Ramírez, F., Schelhorn, S.-E., Lengauer, T., & Albrecht, M. (2008). Computing topological parameters of biological networks. *Bioinformatics*, 24(2), 282– 284. https://doi.org/10.1093/bioinformatics/btm554

Azam, F., Fenchel, T., Field, J. G., Gray, J., Meyer-Reil, L., & Thingstad, F. (1983). The ecological role of water-column microbes in the sea. *Marine Ecology Progress Series*, 10, 257– 263. https://doi.org/10.3354/meps010257

Azam, F., & Malfatti, F. (2007). Microbial structuring of marine ecosystems. *Nature Reviews Microbiology*, 5(10), 782– 791. https://doi.org/10.1038/nrmicro1747

Baines, S. B., & Pace, M. L. (1991). The production of dissolved organic matter by phytoplankton and its importance to bacteria: Patterns across marine and freshwater systems. *Limnology and Oceanography*, 36(6), 1078– 1090. https://doi.org/10.4319/lo.1991.36.6.1078

Baltar, F., Palovaara, J., Vila-Costa, M., Salazar, G., Calvo, E., Pelejero, C., Marrasé, C., Gasol, J. M., & Pinhassi, J. (2015). Response of rare, common and abundant bacterioplankton to anthropogenic perturbations in a Mediterranean coastal site. *FEMS Microbiology Ecology*, 91(6). https://doi.org/10.1093/femsec/fiv058

Beaufort, L., Probert, I., De Garidel-Thoron, T., Bendif, E. M., Ruiz-Pino, D., Metzl, N., Goyet, C., Buchet, N., Coupel, P., Grelaud, M., & Rost, B. (2011). Sensitivity of coccolithophores to carbonate chemistry and ocean acidification. *Nature*, 476(7358), 80– 83. https://doi.org/10.1038/nature10295

Beman, J. M., Chow, C.-E., King, A. L., Feng, Y., Fuhrman, J. A., Andersson, A., Bates, N. R., Popp, B. N., & Hutchins, D. A. (2011). Global declines in oceanic nitrification rates as a consequence of ocean acidification. *Proceedings of the National Academy of Sciences*, 108(1), 208– 213. https://doi.org/10.1073/pnas.1011053108

Beman, J. M., Roberts, K. J., Wegley, L., Rohwer, F., & Francis, C. A. (2007). Distribution and diversity of archaeal ammonia monooxygenase genes associated with corals. *Applied and Environmental Microbiology*, 73(17), 5642– 5647. https://doi.org/10.1128/AEM.00461-07

Bowen, J. L., Kearns, P. J., Holcomb, M., & Ward, B. B. (2013). Acidification alters the composition of ammonia-oxidizing microbial assemblages in marine mesocosms. *Marine Ecology Progress Series*, 492, 1– 8. https://doi.org/10.3354/meps10526

Brown, M. V., Lauro, F. M., Demaere, M. Z., Muir, L., Wilkins, D., Thomas, T., Riddle, M. J., Fuhrman, J. A., Andrews-Pfannkoch, C., Hoffman, J. M., & McQuaid, J. B. (2012). Global biogeography of SAR11 marine bacteria. *Molecular Systems Biology*, 8, 595.

Bunse, C., Lundin, D., Karlsson, C. M., Akram, N., Vila-Costa, M., Palovaara, J., Svensson, L., Holmfeldt, K., González, J. M., Calvo, E., & Pelejero, C. (2016). Response of marine bacterioplankton pH homeostasis gene expression to elevated CO_2. *Nature Climate Change*, 6(5), 483– 487. https://doi.org/10.1038/nclimate2914

Burrell, T., Maas, E., Teesdale-Spittle, P., & Law, C. (2015). Optimising methodology for determining the effect of ocean acidification on bacterial extracellular enzymes. *Biogeosciences Discussions*, 12(8), 5841– 5870. https://doi.org/10.5194/bgd-12-5841-2015

Caldeira, K., & Wickett, M. E. (2003). Oceanography: Anthropogenic carbon and ocean pH. *Nature*, 425(6956), 365– 365. https://doi.org/10.1038/425365a

Carreira, C., Heldal, M., & Bratbak, G. (2013). Effect of increased pCO_2 on phytoplankton–virus interactions. *Biogeochemistry*, 114(1-3), 391– 397. https://doi.org/10.1007/s10533-011-9692-x

Celussi, M., Malfatti, F., Annalisa, F., Gazeau, F., Giannakourou, A., Pitta, P., Tsiola, A., & del Negro, P. (2017). Ocean acidification effect on prokaryotic metabolism tested in two diverse trophic regimes in the Mediterranean Sea. *Estuarine, Coastal and Shelf Science*, 186, 125– 138. https://doi.org/10.1016/j.ecss.2015.08.015

Cox, P. M., Betts, R. A., Jones, C. D., Spall, S. A., & Totterdell, I. J. (2000). Acceleration of global warming due to carbon-cycle feedbacks in a coupled climate model. *Nature*, 408(6809), 184– 187. https://doi.org/10.1038/35041539

Crawfurd, K. J., Alvarez-Fernandez, S., Mojica, K. D., Riebesell, U., & Brussaard, C. P. (2017). Alterations in microbial community composition with increasing fCO_2: A mesocosm study in the eastern Baltic Sea. *Biogeosciences*, 14(16), 3831– 3849. https://doi.org/10.5194/bg-14-3831-2017

De Kluijver, A., Soetaert, K., Schulz, K., Riebesell, U., Bellerby, R., & Middelburg, J. (2010). Phytoplankton-bacteria coupling under elevated CO_2 levels: A stable isotope labelling study. *Biogeosciences*, 7(11), 3783– 3797. https://doi.org/10.5194/bg-7-3783-2010

Deng, W., Wang, Y., Liu, Z., Cheng, H., & Xue, Y. (2014). Hemi: A toolkit for illustrating heatmaps. *PLoS ONE*, 9(11), e111988. https://doi.org/10.1371/journal.pone.0111988

Deng, Y., Jiang, Y.-H., Yang, Y., He, Z., Luo, F., & Zhou, J. (2012). Molecular ecological network analyses. *BMC Bioinformatics*, 13, 1– 20.

Dore, J. E., Lukas, R., Sadler, D. W., Church, M. J., & Karl, D. M. (2009). Physical and biogeochemical modulation of ocean acidification in the central North Pacific. *Proceedings of the National Academy of Sciences*, 106(30), 12,235– 12,240. https://doi.org/10.1073/pnas.0906044106

Eisen, M. B., Spellman, P. T., Brown, P. O., & Botstein, D. (1998). Cluster analysis and display of genome-wide expression patterns. *Proceedings of the National Academy of Sciences*, 95(25), 14,863– 14,868. https://doi.org/10.1073/pnas.95.25.14863

Endres, S., Galgani, L., Riebesell, U., Schulz, K.-G., & Engel, A. (2014). Stimulated bacterial growth under elevated pCO_2: Results from an off-shore mesocosm study. *PLoS ONE*, 9(6), e99228. https://doi.org/10.1371/journal.pone.0099228

Engel, A., Thoms, S., Riebesell, U., Rochelle-Newall, E., & Zondervan, I. (2004). Polysaccharide aggregation as a potential sink of marine dissolved organic carbon. *Nature*, 428(6986), 929– 932. https://doi.org/10.1038/nature02453

Francis, C. A., Beman, J. M., & Kuypers, M. M. (2007). New processes and players in the nitrogen cycle: The microbial ecology of anaerobic and archaeal ammonia oxidation. *The ISME Journal*, 1(1), 19– 27. https://doi.org/10.1038/ismej.2007.8

Fuhrman, J. A. (1999). Marine viruses and their biogeochemical and ecological effects. *Nature*, 399(6736), 541– 548. https://doi.org/10.1038/21119

Galgani, L., Stolle, C., Endres, S., Schulz, K. G., & Engel, A. (2014). Effects of ocean acidification on the biogenic composition of the sea-surface microlayer: Results from a mesocosm study. *Journal of Geophysical Research: Oceans*, 119, 7911– 7924. https://doi.org/10.1002/2014JC010188

Gómez-Pereira, P. R., Hartmann, M., Grob, C., Tarran, G. A., Martin, A. P., Fuchs, B. M., Scanlan, D. J., & Zubkov, M. V. (2013). Comparable light stimulation of organic nutrient uptake by SAR11 and *Prochlorococcus* in the North Atlantic subtropical gyre. *The ISME Journal*, 7(3), 603– 614. https://doi.org/10.1038/ismej.2012.126

Grossart, H.-P., Allgaier, M., Passow, U., & Riebesell, U. (2006). Testing the effect of CO_2 concentration on dynamics of marine heterotrophic bacterioplankton. *Limnology and Oceanography*, 51(1), 1– 11. https://doi.org/10.4319/lo.2006.51.1.0001

Grote, J., Thrash, J. C., Huggett, M. J., Landry, Z. C., Carini, P., Giovannoni, S. J., & Rappé, M. S. (2012). Streamlining and core genome conservation among highly divergent members of the SAR11 clade. *MBio*, 3, e00252– e00212.

Hall-Spencer, J. M., Rodolfo-Metalpa, R., Martin, S., Ransome, E., Fine, M., Turner, S. M., Rowley, S. J., Tedesco, D., & Buia, M. C. (2008). Volcanic carbon dioxide vents show ecosystem effects of ocean acidification. *Nature*, 454(7200), 96– 99. https://doi.org/10.1038/nature07051

Hartmann, M., Hill, P. G., Tynan, E., Achterberg, E. P., Leakey, R. J. G., & Zubkov, M. V. (2016). Resilience of SAR11 bacteria to rapid acidification in

the high-latitude open ocean. *FEMS Microbiology Ecology*, 92(2fiv161). https://doi.org/10.1093/femsec/fiv161

Hoegh-Guldberg, O., Mumby, P., Hooten, A., Steneck, R. S., Greenfield, P., Gomez, E., Harvell, C. D., Sale, P. F., Edwards, A. J., Caldeira, K., & Knowlton, N. (2007). Coral reefs under rapid climate change and ocean acidification. *Science*, 318(5857), 1737– 1742. https://doi.org/10.1126/science.1152509

Hofmann, G. E., Barry, J. P., Edmunds, P. J., Gates, R. D., Hutchins, D. A., Klinger, T., & Sewell, M. A. (2010). The effect of ocean acidification on calcifying organisms in marine ecosystems: An organism-to-ecosystem perspective. *Annual Review of Ecology, Evolution, and Systematics*, 41(1), 127– 147. https://doi.org/10.1146/annurev.ecolsys.110308.120227

Hong, H., Shen, R., Zhang, F., Wen, Z., Chang, S., Lin, W., Kranz, S. A., Luo, Y. W., Kao, S. J., Morel, F. M. M., & Shi, D. (2017). The complex effects of ocean acidification on the prominent N_2-fixing cyanobacterium Trichodesmium. *Science*, 356(6337), 527– 531. https://doi.org/10.1126/science.aal2981

Hoppe, C. J. M., Wolf, K. K., Schuback, N., Tortell, P. D., & Rost, B. (2018). Compensation of ocean acidification effects in Arctic phytoplankton assemblages. *Nature Climate Change*, 8(6), 529– 533. https://doi.org/10.1038/s41558-018-0142-9

Hornick, T., Bach, L. T., Crawfurd, K. J., Spilling, K., Achterberg, E. P., Woodhouse, J. N., Schulz, K. G., Brussaard, C. P. D., Riebesell, U., & Grossart, H. P. (2017). Ocean acidification impacts bacteria—Phytoplankton coupling at low-nutrient conditions. *Biogeosciences*, 14(1), 1– 15. https://doi.org/10.5194/bg-14-1-2017

Hutchins, D. A., Fu, F.-X., Zhang, Y., Warner, M. E., Feng, Y., Portune, K., Bernhardt, P. W., & Mulholland, M. R. (2007). CO_2 control of Trichodesmium N_2 fixation, photosynthesis, growth rates, and elemental ratios: Implications for past, present, and future ocean biogeochemistry. *Limnology and Oceanography*, 52(4), 1293– 1304. https://doi.org/10.4319/lo.2007.52.4.1293

Hutchins, D. A., Mulholland, M. R., & Fu, F. (2009). Nutrient cycles and marine microbes in a CO_2-enriched ocean. *Oceanography*, 22(4), 128– 145. https://doi.org/10.5670/oceanog.2009.103

Jiao, N., Herndl, G. J., Hansell, D. A., Benner, R., Kattner, G., Wilhelm, S. W., Kirchman, D. L., Weinbauer, M. G., Luo, T., Chen, F., & Azam, F. (2010). Microbial production of recalcitrant dissolved organic matter: Long-term carbon storage in the global ocean. *Nature Reviews Microbiology*, 8(8), 593– 599. https://doi.org/10.1038/nrmicro2386

Jiao, N., & Zheng, Q. (2011). The microbial carbon pump: From genes to ecosystems. *Applied and Environmental Microbiology*, 77(21), 7439– 7444. https://doi.org/10.1128/AEM.05640-11

Joint, I., Doney, S. C., & Karl, D. M. (2010). Will ocean acidification affect marine microbes? *The ISME Journal*, 5, 1– 7.

Joos, F., Plattner, G.-K., Stocker, T. F., Marchal, O., & Schmittner, A. (1999). Global warming and marine carbon cycle feedbacks on future atmospheric CO_2. *Science*, 284(5413), 464– 467. https://doi.org/10.1126/science.284.5413.464

Karl, D., Letelier, R., Tupas, L., Dore, J., Christian, J., & Hebel, D. (1997). The role of nitrogen fixation in biogeochemical cycling in the subtropical North Pacific Ocean. *Nature*, 388(6642), 533– 538. https://doi.org/10.1038/41474

Kim, J.-M., Lee, K., Yang, E. J., Shin, K., Noh, J. H., Park, K. T., Hyun, B., Jeong, H. J., Kim, J. H., Kim, K. Y., Kim, M., Kim, H. C., Jang, P. G., & Jang, M. C. (2010). Enhanced production of oceanic dimethylsulfide resulting from CO_2-induced grazing activity in a high CO_2 world. *Environmental Science &Technology*, 44(21), 8140– 8143. https://doi.org/10.1021/es102028k

Kirchman, D., K'nees, E., & Hodson, R. (1985). Leucine incorporation and its potential as a measure of protein synthesis by bacteria in natural aquatic systems. *Applied and Environmental Microbiology*, 49(3), 599– 607.

Krause, E., Wichels, A., Giménez, L., Lunau, M., Schilhabel, M. B., & Gerdts, G. (2012). Small changes in pH have direct effects on marine bacterial community composition: A microcosm approach. *PLoS ONE*, 7(10), e47035. https://doi.org/10.1371/journal.pone.0047035

Larsen, J., Larsen, A., Thyrhaug, R., Bratbak, G., & Sandaa, R.-A. (2008). Response of marine viral populations to a nutrient induced phytoplankton bloom at different pCO_2 levels. *Biogeosciences*, 5(2), 523– 533. https://doi.org/10.5194/bg-5-523-2008

Le Quéré, C., Andrew, R. M., Canadell, J. G., Sitch, S., Korsbakken, J. I., Peters, G. P., Manning, A. C., Boden, T. A., Tans, P. P., Houghton, R. A., & Keeling, R. F. (2016). Global carbon budget 2016. *Earth System Science Data*, 8(2), 605– 649. https://doi.org/10.5194/essd-8-605-2016

Lebaron, P., Servais, P., Baudoux, A.-C., Bourrain, M., Courties, C., & Parthuisot, N. (2002). Variations of bacterial-specific activity with cell size and nucleic acid content assessed by flow cytometry. *Aquatic Microbial Ecology*, 28, 131– 140. https://doi.org/10.3354/ame028131

Levitan, O., Rosenberg, G., Setlik, I., Setlikova, E., Grigel, J., Klepetar, J., Prasil, O., & Berman-Frank, I. (2007). Elevated CO_2 enhances nitrogen fixation and growth in the marine cyanobacterium *Trichodesmium*. *Global Change Biology*, 13(2), 531– 538. https://doi.org/10.1111/j.1365-2486.2006.01314.x

Lindh, M. V., Riemann, L., Baltar, F., Romero-Oliva, C., Salomon, P. S., Granéli, E., & Pinhassi, J. (2013). Consequences of increased temperature and acidification on bacterioplankton community composition during a

mesocosm spring bloom in the Baltic Sea. *Environmental Microbiology Reports*, 5(2), 252– 262. https://doi.org/10.1111/1758-2229.12009

Liu, J., Weinbauer, M. G., Maier, C., Dai, M., & Gattuso, J.-P. (2010). Effect of ocean acidification on microbial diversity and on microbe-driven biogeochemistry and ecosystem functioning. *Aquatic Microbial Ecology*, 61(3), 291– 305. https://doi.org/10.3354/ame01446

Maas, E. W., Law, C. S., Hall, J. A., Pickmere, S., Currie, K. I., Chang, F. H., Voyles, K. M., & Caird, D. (2013). Effect of ocean acidification on bacterial abundance, activity and diversity in the Ross Sea, Antarctica. *Aquatic Microbial Ecology*, 70(1), 1– 15. https://doi.org/10.3354/ame01633

Maier-Reimer, E., & Hasselmann, K. (1987). Transport and storage of CO_2 in the ocean—An inorganic ocean-circulation carbon cycle model. *Climate Dynamics*, 2(2), 63– 90. https://doi.org/10.1007/BF01054491

Marie, D., Partensky, F., Jacquet, S., & Vaulot, D. (1997). Enumeration and cell cycle analysis of natural populations of marine picoplankton by flow cytometry using the nucleic acid stain SYBR Green I. *Applied and Environmental Microbiology*, 63(1), 186– 193.

Merbt, S. N., Stahl, D. A., Casamayor, E. O., Martí, E., Nicol, G. W., & Prosser, J. I. (2012). Differential photoinhibition of bacterial and archaeal ammonia oxidation. *FEMS Microbiology Letters*, 327(1), 41– 46. https://doi.org/10.1111/j.1574-6968.2011.02457.x

Meron, D., Atias, E., Kruh, L. I., Elifantz, H., Minz, D., Fine, M., & Banin, E. (2011). The impact of reduced pH on the microbial community of the coral Acropora eurystoma. *The ISME Journal*, 5(1), 51– 60. https://doi.org/10.1038/ismej.2010.102

Messer, L. F., Mahaffey, C., Robinson, C. M., Jeffries, T. C., Baker, K. G., Bibiloni Isaksson, J., Ostrowski, M., Doblin, M. A., Brown, M. V., & Seymour, J. R. (2016). High levels of heterogeneity in diazotroph diversity and activity within a putative hotspot for marine nitrogen fixation. *The ISME Journal*, 10(6), 1499– 1513. https://doi.org/10.1038/ismej.2015.205

Moisander, P. H., Benavides, M., Bonnet, S., Berman-Frank, I., White, A. E., & Riemann, L. (2017). Chasing after non-cyanobacterial nitrogen fixation in marine pelagic environments. *Frontiers in Microbiology*, 8, 1736. https://doi.org/10.3389/fmicb.2017.01736

Montoya, J. P., Holl, C. M., Zehr, J. P., Hansen, A., Villareal, T. A., & Capone, D. G. (2004). High rates of N_2 fixation by unicellular diazotrophs in the oligotrophic Pacific Ocean. *Nature*, 430(7003), 1027– 1032. https://doi.org/10.1038/nature02824

Newbold, L. K., Oliver, A. E., Booth, T., Tiwari, B., DeSantis, T., Maguire, M., Andersen, G., van der Gast, C. J., & Whiteley, A. S. (2012). The response of marine picoplankton to ocean acidification. *Environmental Microbiology*, 14(9), 2293– 2307. https://doi.org/10.1111/j.1462-2920.2012.02762.x

Newman, M. E. J. (2006). Finding community structure in networks using the eigenvectors of matrices. *Physical Review E*, 74, 1– 19.

Oksanen, J., Kindt, R., Legendre, P., O'hara, B., Stevens, M. H. H., Oksanen, M. J., & Suggests, M. (2007). The vegan package. *Community ecology package*, 10, 631– 637.

Olesen, J. M., Bascompte, J., Dupont, Y. L., & Jordano, P. (2007). The modularity of pollination networks. *Proceedings of the National Academy of Sciences*, 104(50), 19,891– 19,896. https://doi.org/10.1073/pnas.0706375104

Pakulski, J. D., & Benner, R. (1994). Abundance and distribution of carbohydrates in the ocean. *Limnology and Oceanography*, 39(4), 930– 940. https://doi.org/10.4319/lo.1994.39.4.0930

Parks, D. H., Tyson, G. W., Hugenholtz, P., & Beiko, R. G. (2014). STAMP: Statistical analysis of taxonomic and functional profiles. *Bioinformatics*, 30(21), 3123– 3124. https://doi.org/10.1093/bioinformatics/btu494

Piontek, J., Borchard, C., Sperling, M., Schulz, K. G., Riebesell, U., & Engel, A. (2013). Response of bacterioplankton activity in an Arctic fjord system to elevated pCO_2: Results from a mesocosm perturbation study. *Biogeosciences*, 10(1), 297– 314. https://doi.org/10.5194/bg-10-297-2013

Piontek, J., Lunau, M., Handel, N., Borchard, C., Wurst, M., & Engel, A. (2010). Acidification increases microbial polysaccharide degradation in the ocean. *Biogeosciences*, 7(5), 1615– 1624. https://doi.org/10.5194/bg-7-1615-2010

Qin, W., Amin, S. A., Martens-Habbena, W., Walker, C. B., Urakawa, H., Devol, A. H., Ingalls, A. E., Moffett, J. W., Armbrust, E. V., & Stahl, D. A. (2014). Marine ammonia-oxidizing archaeal isolates display obligate mixotrophy and wide ecotypic variation. *Proceedings of the National Academy of Sciences*, 111(34), 12,504– 12,509. https://doi.org/10.1073/pnas.1324115111

Raven, J., Caldeira, K., Elderfield, H., Hoegh-Guldberg, O., Liss, P., Riebesell, U., Shepherd, J., Turley, C., & Watson, A. (2005). *Ocean acidification due to increasing atmospheric carbon dioxide*. London: The Royal Society.

Ray, J. L., Töpper, B., An, S., Silyakova, A., Spindelböck, J., Thyrhaug, R., DuBow, M. S., Thingstad, T. F., & Sandaa, R. A. (2012). Effect of increased pCO_2 on bacterial assemblage shifts in response to glucose addition in Fram Strait seawater mesocosms. *FEMS Microbiology Ecology*, 82(3), 713– 723. https://doi.org/10.1111/j.1574-6941.2012.01443.x

Rees, A. P., Turk-Kubo, K. A., Al-Moosawi, L., Alliouane, S., Gazeau, F., Hogan, M. E., & Zehr, J. P. (2017). Ocean acidification impacts on nitrogen fixation in the coastal western Mediterranean Sea. *Estuarine, Coastal and Shelf Science*, 186, 45– 57. https://doi.org/10.1016/j.ecss.2016.01.020

Reshef, Y. A., Reshef, D. N., Finucane, H. K., Sabeti, P. C., & Mitzenmacher, M. (2016). Measuring dependence powerfully and equitably. *Journal of Machine Learning Research*, 17, 1– 63.

Riebesell, U., Schulz, K. G., Bellerby, R. G. J., Botros, M., Fritsche, P., Meyerhöfer, M., Neill, C., Nondal, G., Oschlies, A., Wohlers, J., & Zöllner, E. (2007). Enhanced biological carbon consumption in a high CO_2 ocean. *Nature*, 450(7169), 545– 548. https://doi.org/10.1038/nature06267

Rodolfo-Metalpa, R., Houlbrèque, F., Tambutté, É., Boisson, F., Baggini, C., Patti, F. P., Jeffree, R., Fine, M., Foggo, A., Gattuso, J. P., & Hall-Spencer, J. M. (2011). Coral and mollusc resistance to ocean acidification adversely affected by warming. *Nature Climate Change*, 1(6), 308– 312. https://doi.org/10.1038/nclimate1200

Roy, A.-S., Gibbons, S. M., Schunck, H., Owens, S., Caporaso, J. G., Sperling, M., Nissimov, J. I., Romac, S., Bittner, L., Mühling, M., Riebesell, U., LaRoche, J., & Gilbert, J. A. (2013). Ocean acidification shows negligible impacts on high-latitude bacterial community structure in coastal pelagic mesocosms. *Biogeosciences*, 10(1), 555– 566. https://doi.org/10.5194/bg-10-555-2013

Sala, M. M., Aparicio, F. L., Balagué, V., Boras, J. A., Borrull, E., Cardelús, C., Cros, L., Gomes, A., López-Sanz, A., Malits, A., & Martínez, R. A. (2015). Contrasting effects of ocean acidification on the microbial food web under different trophic conditions. *ICES Journal of Marine Science*, 73, 670– 679.

Schloss, P. D., Westcott, S. L., Ryabin, T., Hall, J. R., Hartmann, M., Hollister, E. B., Lesniewski, R. A., Oakley, B. B., Parks, D. H., Robinson, C. J., Sahl, J. W., Stres, B., Thallinger, G. G., van Horn, D. J., & Weber, C. F. (2009). Introducing mothur: Open-source, platform-independent, community-supported software for describing and comparing microbial communities. *Applied and Environmental Microbiology*, 75(23), 7537– 7541. https://doi.org/10.1128/AEM.01541-09

Shakun, J. D., Clark, P. U., He, F., Marcott, S. A., Mix, A. C., Liu, Z., Otto-Bliesner, B., Schmittner, A., & Bard, E. (2012). Global warming preceded by increasing carbon dioxide concentrations during the last deglaciation. *Nature*, 484(7392), 49– 54. https://doi.org/10.1038/nature10915

Shannon, P., Markiel, A., Ozier, O., Baliga, N. S., Wang, J. T., Ramage, D., Amin, N., Schwikowski, B., & Ideker, T. (2003). Cytoscape: A software environment for integrated models of biomolecular interaction networks. *Genome Research*, 13(11), 2498– 2504. https://doi.org/10.1101/gr.1239303

Shi, D., Xu, Y., Hopkinson, B. M., & Morel, F. M. (2010). Effect of ocean acidification on iron availability to marine phytoplankton. *Science*, 327(5966), 676– 679. https://doi.org/10.1126/science.1183517

Siu, N., Apple, J. K., & Moyer, C. L. (2014). The effects of ocean acidity and elevated temperature on bacterioplankton community structure and

metabolism. *Open Journal of Ecology*, 04(08), 434– 455. https://doi.org/10.4236/oje.2014.48038

Stocker, T. (2014). *Climate Change 2013: The Physical Science Basis: Working Group I Contribution to the Fifth Assessment Report of the Intergovernmental Panel on Climate Change*. Cambidge: Cambridge University Press.

Tait, K., Laverock, B., & Widdicombe, S. (2014). Response of an arctic sediment nitrogen cycling community to increased CO_2. *Estuaries and Coasts*, 37(3), 724– 735. https://doi.org/10.1007/s12237-013-9709-x

Tatters, A. O., Roleda, M. Y., Schnetzer, A., Fu, F., Hurd, C. L., Boyd, P. W., Caron, D. A., Lie, A. A. Y., Hoffmann, L. J., & Hutchins, D. A. (2013). Short-and long-term conditioning of a temperate marine diatom community to acidification and warming. *Philosophical Transactions of the Royal Society B: Biological Sciences*, 368, 20120437(1627). https://doi.org/10.1098/rstb.2012.0437

Teira, E., Fernández, A., Álvarez-Salgado, X. A., García-Martín, E. E., Serret, P., & Sobrino, C. (2012). Response of two marine bacterial isolates to high CO_2 concentration. *Marine Ecology Progress Series*, 453, 27– 36. https://doi.org/10.3354/meps09644

Thomas, P. C., Tajeddine, R., Tiscareno, M. S., Burns, J. A., Joseph, J., Loredo, T. J., Helfenstein, P., & Porco, C. (2016). Enceladus's measured physical libration requires a global subsurface ocean. *Icarus*, 264, 37– 47. https://doi.org/10.1016/j.icarus.2015.08.037

Traving, S. J., Clokie, M. R., & Middelboe, M. (2014). Increased acidification has a profound effect on the interactions between the cyanobacterium *Synechococcus* sp. WH7803 and its viruses. *FEMS Microbiology Ecology*, 87(1), 133– 141. https://doi.org/10.1111/1574-6941.12199

Tu, Q., Yu, H., He, Z., Deng, Y., Wu, L., van Nostrand, J., Zhou, A., Voordeckers, J., Lee, Y. J., Qin, Y., Hemme, C. L., Shi, Z., Xue, K., Yuan, T., Wang, A., & Zhou, J. (2014). GeoChip 4: A functional gene-array-based high-throughput environmental technology for microbial community analysis. *Molecular Ecology Resources*, 14(5), 914– 928. https://doi.org/10.1111/1755-0998.12239

Wang, Y., Zhang, R., Zheng, Q., Deng, Y., Van Nostrand, J. D., Zhou, J., & Jiao, N. (2015). Bacterioplankton community resilience to ocean acidification: Evidence from microbial network analysis. *ICES Journal of Marine Science*, 73(3), 865– 875. fsv187

Wannicke, N., Endres, S., Engel, A., Grossart, H.-P., Nausch, M., Unger, J., & Voss, M. (2012). Response of Nodularia spumigena to pCO_2—Part 1: Growth, production and nitrogen cycling. *Biogeosciences*, 9(8), 2973– 2988. https://doi.org/10.5194/bg-9-2973-2012

Watson, A. J., Schuster, U., Bakker, D. C. E., Bates, N. R., Corbiere, A., Gonzalez-Davila, M., Friedrich, T., Hauck, J., Heinze, C., Johannessen, T., Kortzinger, A., Metzl, N., Olafsson, J., Olsen, A., Oschlies, A., Padin, X. A., Pfeil, B., Santana-Casiano, J. M., Steinhoff, T., Telszewski, M., Rios, A. F., Wallace, D. W. R., & Wanninkhof, R. (2009). Tracking the variable North Atlantic sink for atmospheric CO_2. *Science*, 326(5958), 1391– 1393. https://doi.org/10.1126/science.1177394

Weinbauer, M. G., Mari, X., & Gattuso, J.-P. (2011). *Effect of ocean acidification on the diversity and activity of heterotrophic marine microorganisms. Ocean acidification* (pp. 83– 98). Oxford: Oxford University Press.

Westwood, K., Thomson, P., Van Den Enden, R., Maher, L., Wright, S., & Davidson, A. (2018). Ocean acidification impacts primary and bacterial production in Antarctic coastal waters during austral summer. *Journal of Experimental Marine Biology and Ecology*, 498, 46– 60. https://doi.org/10.1016/j.jembe.2017.11.003

Witt, V., Wild, C., Anthony, K., Diaz-Pulido, G., & Uthicke, S. (2011). Effects of ocean acidification on microbial community composition of, and oxygen fluxes through, biofilms from the Great Barrier Reef. *Environmental Microbiology*, 13(11), 2976– 2989. https://doi.org/10.1111/j.1462-2920.2011.02571.x

Yamada, N., & Suzumura, M. (2010). Effects of seawater acidification on hydrolytic enzyme activities. *Journal of Oceanography*, 66(2), 233– 241. https://doi.org/10.1007/s10872-010-0021-0

Zhang, R., Xia, X., Lau, S. C. K., Motegi, C., Weinbauer, M. G., & Jiao, N. (2013). Response of bacterioplankton community structure to an artificial gradient of pCO_2 in the Arctic Ocean. *Biogeosciences*, 10(6), 3679– 3689. https://doi.org/10.5194/bg-10-3679-2013

Zhou, J., Deng, Y., Luo, F., He, Z., Tu, Q., & Zhi, X. (2010). Functional molecular ecological networks. *mBio*, 1,e00169-10(4). https://doi.org/10.1128/mBio.00169-10